A folding reaction at the C-terminal domain drives temperature sensing in TRPM8 channels

Ignacio Díaz-Franulic[a,b,1], Natalia Raddatz[a,2], Karen Castillo[a], Fernando D. González-Nilo[a,b], and Ramon Latorre[a,1]

[a]Centro Interdisciplinario de Neurociencia de Valparaíso, Facultad de Ciencias, Universidad de Valparaíso, Valparaíso, Chile, 2340000; and [b]Center for Bioinformatics and Integrative Biology, Facultad de Ciencias de la Vida, Universidad Andrés Bello, Santiago, Chile, 8370146

Contributed by Ramón Latorre, June 18, 2020 (sent for review March 9, 2020; reviewed by Feng Qin and Thomas Voets)

In mammals, temperature-sensitive TRP channels make membrane conductance of cells extremely temperature dependent, allowing the detection of temperature ranging from noxious cold to noxious heat. We progressively deleted the distal carboxyl terminus domain (CTD) of the cold-activated melastatin receptor channel, TRPM8. We found that the enthalpy change associated with channel gating is proportional to the length of the CTD. Deletion of the last 36 amino acids of the CTD transforms TRPM8 into a reduced temperature-sensitivity channel (Q_{10} ~4). Exposing the intracellular domain to a denaturing agent increases the energy required to open the channel indicating that cold drives channel gating by stabilizing the folded state of the CTD. Experiments in the presence of an osmoticant agent suggest that channel gating involves a change in solute-inaccessible volume in the CTD of ~1,900 Å^3. This volume matches the void space inside the coiled coil according to the cryogenic electron microscopy structure of TRPM8. The results indicate that a folding–unfolding reaction of a specialized temperature-sensitive structure is coupled to TRPM8 gating.

TRPM8 | temperature sensor | heat capacity | coiled coil | protein folding

Thermo-TRP channels are a subset of ion channels of the Transient Receptor Potential (TRP) superfamily whose activity exhibits unusually large temperature dependence, making them a cornerstone in diverse physiological responses (1–3). The TRP Melastatin 8 (TRPM8) ion channel is a cationic-nonselective cold receptor widely expressed in the somatosensory system but that has also been found in various other tissues such as liver, bladder, the male genital tract, muscle, and lung (4). As a bona fide temperature-sensitive protein, its activity increases sharply below 28 °C, reaching the maximal activity ~10 °C (Q_{10} > 20). Channel gating is also controlled by voltage (5), PIP2 (6, 7) and is activated by cooling agents such as menthol and icillin (8). The recently solved TRPM8 channel structure shows a tetrameric arrangement with the permeation pathway at the channel symmetry axis and two narrow constrictions at the inner pore end that constitute the channel activation gate (9). Each channel subunit consists of six membrane-spanning segments, a large amino terminus (NTD), and carboxyl terminus domain (CTD). The NTD (~700 amino acids) contains four Melastatin Homology Regions (MHRs), and the CTD comprises a conserved amino acid sequence known as the TRP box and a 24-residue-length tetrameric coiled coil domain that is important for channel assembly, trafficking, and function (10). Although the structure of several thermo-TRP channels has been elucidated in several conformations by single-particle cryogenic electron microscopy (spCryo-EM) (9, 11–15), both the structural and physicochemical bases underlying their temperature sensitive gating remain obscure (2, 16, 17). The search of a dedicated temperature-sensing domain has been unsuccessful since mutations that severely impact the channel temperature dependence are widely distributed across the protein (18). Additionally, it has also been proposed that a dedicated temperature sensor is unnecessary, as long as the protein experiences a large change in the molar heat capacity during the closed–open transition (19, 20). Although coiled coil assembles have been shown to play a role in setting the temperature-driven activity of several proteins, including ion channels (21–26), their role in thermo-TRP channel gating has never been assessed to date.

Based on our previous studies that suggested that the CTD of TRPM8 is involved in temperature sensing (27), we characterized the temperature dependence of TRPM8 wild-type (WT) channels and that of three variants whose CTD—enclosing a coiled coil domain—was progressively deleted. We found that the enthalpy change (ΔH) during channel activation is proportional to the CTD length and that removal of the last 36 amino acids of the CTD (TRPM8ΔCT36) renders the channel with a temperature sensitivity notably reduced. In order to assess the predictions of the molar heat capacity hypothesis we exposed the internal aspect of TPM8 to a denaturing agent expecting to reveal the existence of a temperature-dependent folding or unfolding reaction during channel gating. We found that urea stabilized the closed state of WT channels but did not affected the TRPM8ΔCT36 mutant (Q_{10} ~4), suggesting that temperature-dependent gating in the TRPM8 channel arises from a cold-driven stabilization of the CTD in its folded state. Additionally, by performing experiments in hyperosmotic conditions we determined the temperature-dependent change in the solute-inaccessible aqueous volume of the distal CTD, a result

Significance

Sensory and homeostatic responses in several organisms depend on the exquisite temperature dependence of ion channels of the transient receptor potential family (thermo-TRP). To date, this temperature dependence has been explained either in terms of the existence of a dedicated temperature sensor or by the increase in the molar heat capacity during channel gating. We found that the Carboxy Terminus Domain (CTD) is required for temperature-driven gating of the cold-activated TRPM8 channel and that this domain folds in response to cold. Here we propose that the CTD of the TRPM8 channel is a bona fide temperature sensor that drives channel gating due to an increase in the molar heat capacity during the folded-to-unfolded transition.

Author contributions: I.D.-F. and R.L. designed research; I.D.-F., N.R., and K.C. performed research; I.D.-F., N.R., K.C., F.G.-N., and R.L. analyzed data; and I.D.-F. and R.L. wrote the paper.

Reviewers: F.Q., State University of New York at Buffalo; and T.V., Katholieke Universiteit Leuven.

The authors declare no competing interest.

[1]To whom correspondence may be addressed. Email: ignacio.diaz@unab.cl, or ramon.latorre@uv.cl.

[2]Present address: Institute of Plant Biochemistry and Photosynthesis, Consejo Superior de Investigaciones Científicas, Universidad de Sevilla, Seville-41092, Spain

This article contains supporting information online at https://www.pnas.org/lookup/suppl/doi:10.1073/pnas.2004303117/-/DCSupplemental.

First published August 3, 2020.

consistent with the void space observed in the channel structure obtained by Cryo-EM. This led us to propose a model where the distal CTD of TRPM8 is a key structural component of the temperature sensor and its cold-induced folding is a pivotal event for the cold-driven gating of the TRPM8 channel.

Results

The C-Terminal Domain Integrity Determines the TRPM8 Temperature Dependence. The CTD of the TRPM8 channel is an interchangeable module that confers cold sensitivity to an otherwise heat receptor such as the TRPV1 channel (27). The CTD contains a TRP domain which is followed by the first CTD helix (CTDH1) and the second CTD helix (CTDH2) and joins the distal coiled coil domain (CC) through a short loop (15). Coiled coils are amphipathic arrangements of α helices that twist around one another and are characterized by a seven-residue periodicity (heptad repeat) of amino acids (***abcdefg***), where ***a*** and ***d*** are hydrophobic and ***e*** and ***g*** are charged or polar, forming a particularly stable structure (28, 29). Even though coiled coils can be found in both membrane-associated and soluble proteins whose activity exhibits substantial temperature dependence (21–27, 30, 31), their role has never been assessed in thermo-TRP channels. Thus, we characterized the temperature dependence of TRPM8 channels whose CTD was periodically truncated in heptads starting at the coiled coil domain up to the linker connecting with the CTD2 as schematized in Fig. 1*A*. Although we generated several truncated channels (Δ8, Δ15, Δ22, Δ29, Δ36, and Δ40), the only voltage-activated channels were TRPM8ΔCT8, TRPM8ΔCT15, and TRPM8ΔCT36. Fig. 1*B* shows the normalized conductance vs. voltage relations (G–V) obtained after patch clamp recording in cell-attached configuration of the TRPM8 WT (32), TRPM8ΔCT8, TRPM8ΔCT15, and TRPM8ΔCT36 channels expressed in *Xenopus* oocytes, at temperatures ranging from 10 to 30 °C. Assuming a two-state model for channel gating, the free energy difference between the closed–open (C–O) states during of channel activation is

$$\Delta G = zFV_o, \quad [1]$$

where z is the channel effective valence [z = 0.7 (32)], F is the Faraday constant, and V_o is the half-maximal activation voltage obtained from the Boltzmann fit of the conductance vs. voltage data shown in Fig. 1*C*. Therefore, the natural logarithm of the apparent equilibrium constant K_{app} of the C–O reaction can be obtained from

$$\ln K_{app} = -\frac{\Delta G}{RT}, \quad [2]$$

where R and T are the Universal Gas constant and temperature in Kelvin degrees, respectively.

Fig. 1*C* shows the natural logarithm of the apparent equilibrium constant ($\ln K_{app}$) plotted against 1,000/T, expressed in K^{-1}. The datasets for each TRPM8 variant were fitted according to the Van't Hoff equation (33)

$$\ln K_{app} = \frac{\Delta H}{R} * \frac{1}{T} + \frac{\Delta S}{R}, \quad [3]$$

where ΔH and ΔS are the enthalpy and entropy changes for the C–O equilibrium obtained from the slope and intercept, respectively. As reported before for the TRPM8 WT channel, we also observed two temperature-dependent processes with different enthalpy changes when plotting the $\ln K_{app}$ − 1/T data. The most pronounced slope of the $\ln Kapp$ − 1/T curve was −61 ± 4 kcal/mol for the WT channels, which progressively decreases after CTD truncation to −21.4 ± 2 kcal/mol in the TRPM8ΔCT36 mutant (Fig. 1*D*). Entropy changes exhibited similar behavior (Fig. 1*E*) starting at 210 ± 10 cal/mol*K for WT channels reaching a minimal value of 80 ± 6 cal/mol*K in the TRPM8ΔCT36 mutant. Whether the deletions are targeting the temperature-sensing machinery or they are uncoupling it from the pore opening is uncertain. However, the additive nature of the ΔH suggests that the former mechanism can explain the results more parsimoniously.

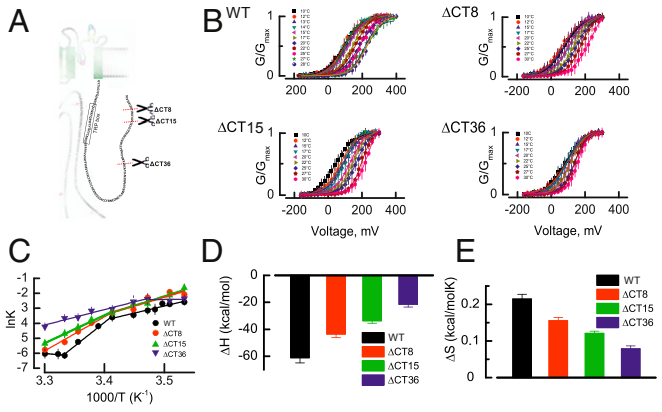

Fig. 1. Thermodynamics of TRPM8 CTD-deleted mutants. (*A*) CTD domain (in blue) and its amino acid sequence. Scissors define the position at which the CTD was deleted in the different mutants tested. (*B*) Normalized conductance vs. voltage relationship (G–V) obtained by patch clamp recording in the cell-attached configuration of the TRPM8 WT (32). TRPM8ΔCT8, TRPM8ΔCT15, and TRPM8ΔCT36 channels at the temperatures indicated. Solid lines are isothermal Boltzmann fits (*SI Appendix*, Eq. S1). (*C*) lnK vs. 1,000/T data for each channel were fitted using the Van't Hoff equation. A linear fit of the data to lnK = ΔH/RT − ΔS/R produced an estimate of the (*D*) enthalpy (ΔH) and (*E*) entropy change (ΔS). Two clearly distinguishable slopes can be appreciated in *C*. The ΔH obtained from the most pronounced slope is plotted for the WT and mutant TRPM8 channels in *D*. Van't Hoff equation fit parameters are shown in *SI Appendix*, Table S1. Error bars are SE, *n* = 6 to 10.

Temperature-Dependent Folding of the CTD of the TRPM8. Clapham and Miller proposed that the unusually large temperature dependence of the thermo-TRP channels gating is a natural consequence of a large change in the molar heat capacity (ΔC_p) during the closed to open transition (19). According to the heat capacity hypothesis both cold and heat activation can be handled as a protein unfolding reaction. If that were correct, a temperature-sensing domain will unfold when exposed to a denaturing agent, decreasing the electrical work required to open the channel, thus shifting to the left the G–V relation. Otherwise, a rightward shift of the G–V relation would indicate that channel opening is accompanied by a folding event. We tested this prediction by exposing the intracellular domain of the TRPM8 channel to urea, a denaturing agent that assists the temperature/pressure-induced unfolding of macromolecules, including DNA and proteins (34). In terms of the interpretation of the results, the most convenient experimental strategy is to assess the effect of urea on the temperature-sensing structure at temperatures where it is more likely to find it in its resting or active states, namely, 30 and 10 °C (32). However, due to membrane seal instability it is difficult to perform patch clamp recordings at high temperature/voltage in the presence of urea. Therefore, to test our hypothesis at higher temperatures we did all of the experiments in the presence of urea at a temperature that is still compatible with patch stability (25 °C). This temperature allowed us to generate G–V curves close enough to saturation to obtain reliable Boltzmann fit parameters. Unspecific effects of urea were estimated by their impact on the gating energetics of the less temperature-dependent variant TRPM8ΔCT36. Fig. 2

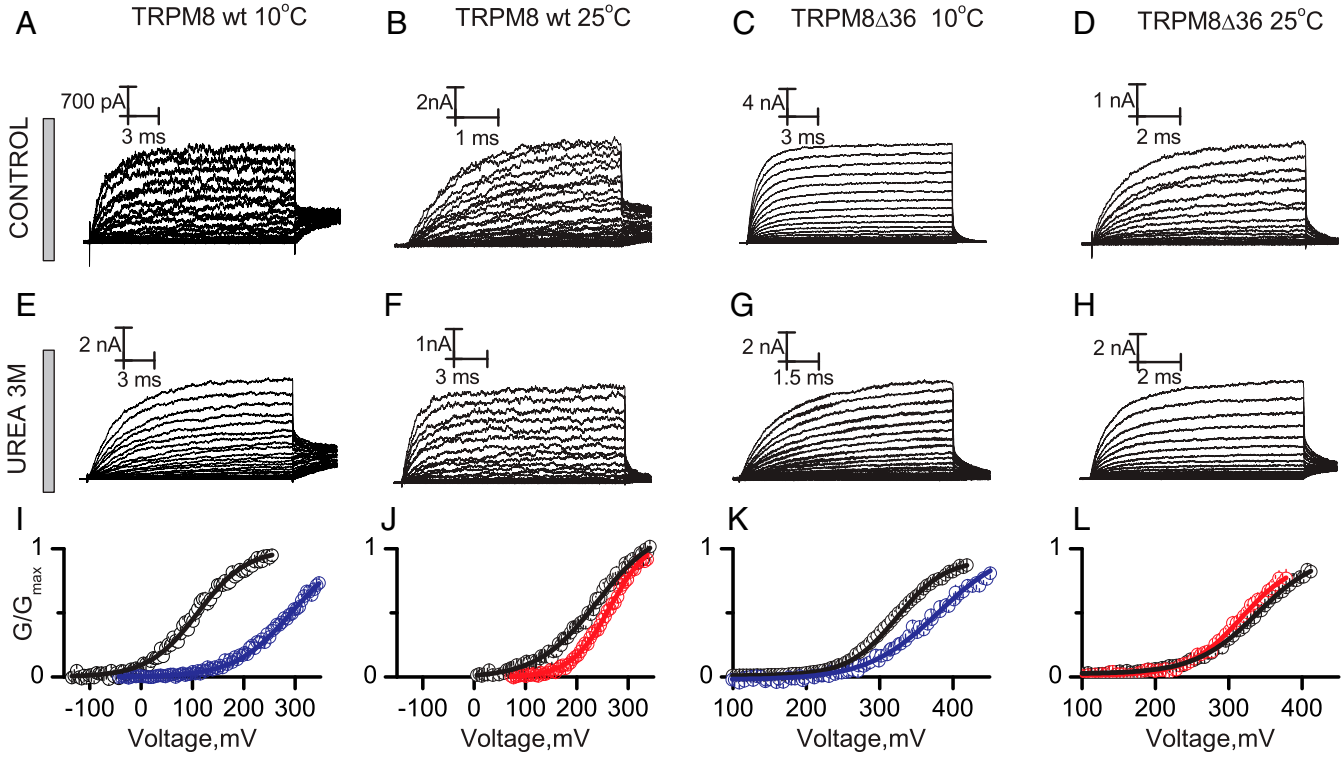

Fig. 2. Effect of a denaturing agent on the temperature-driven gating of TRPM8 channels. Representative recordings of macroscopic currents of TRPM8 and TRPM8ΔCT36 evoked by voltage pulses ranging between −140 and 420 mV (*A–D*) in standard recording solution and (*E–H*) in the presence of 3M urea at the temperature indicated. For the sake of clarity, only one of every two current records is shown in *A–H*. (*I–L*) Average G–V relations in the absence (open black circles) and in the presence of urea (blue open circles are data at 10 °C; red open circles are data at 25 °C) obtained from normalized tail currents, Solid lines are Boltzmann fits to Eq. S1 (*SI Appendix*, Eq. S1). Fit parameters are summarized in *SI Appendix*, Table S2. Detailed voltage protocols are given in *SI Appendix*, Table S3. Error bars are SE, $n = 4$ to 6.

shows current traces evoked by voltage test pulses in membrane patches containing TRPM8 WT and TRPM8ΔCT36 channels recorded in the inside-out configuration under control conditions (Fig. 2 *A–D*) and in the presence of 3M urea in the bath solution (Fig. 2 *E–H*) performed at 10 and 25 °C. The respective G–V curves are shown in Fig. 2 *I–L*. A remarkable result is that urea induces rightward shifts of the G–V curve of the WT channel at 10 and 25 °C by 187 ± 10 and 32 ± 8 mV, respectively, which, considering an effective valence of z = 0.70 (32), represents a closed-state stabilization of 2.90 ± 0.22 and 0.33 ± 0.25 kcal/mol, respectively. The impact of urea on the TRPM8ΔCT36 variant was negligible with 1.00 ± 0.24 and −0.10 ± 0.18 kcal/mol at 10 and 25 °C, respectively. These results suggest the existence of an intracellular, solvent-exposed structure that at low temperatures decreases the energy required to open the channel—a temperature-sensing domain—and that must be folded to accomplish its function.

In order to put these results in a quantitative framework, let us assume that the free energy difference ΔG between the open and closed TRPM8 WT channel is given by

$$\Delta G = \Delta G^{o} + \Delta G^{f}_{U} + zFV, \qquad [4]$$

where ΔG^{f}_{U} is the urea-sensitive free energy difference contributed by the folding/unfolding of the intracellular domain, z is the apparent number of gating charges (32), F is the Faraday constant, and V is the applied voltage. Thus, the urea-sensitive component free energy of folding at a given temperature, ΔG^{f}_{U}, is defined as

$$\Delta G^{f}_{U} = (z * F * V_{o,U}) - (z * F * V_{o,C}), \qquad [5]$$

where $V_{o,U}$ and $V_{o,C}$ are the half-maximal activation voltage, both obtained from the fit of the Boltzmann equation to normalized tail currents amplitude obtained in the presence of urea (U) or control (C) recording solution. If the urea-sensitive component of the free energy of folding ΔG^{f}_{U} exhibits a temperature-dependent behavior ($\Delta\Delta G^{T}_{U}$), it can be obtained from the relation

$$\Delta\Delta G^{T}_{U} = (\Delta G^{10°C}_{U} - \Delta G^{25°C}_{U}), \qquad [6]$$

which is made up by the CTD component ($\Delta\Delta G^{T}_{CTD}$) and that including the contributions of all channel regions outside the CTD ($\Delta\Delta G^{T}_{ch}$),

$$\Delta\Delta G^{T}_{U} = \Delta\Delta G^{T}_{CTD} + \Delta\Delta G^{T}_{ch}. \qquad [7]$$

The $\Delta\Delta G^{T}_{ch}$ can be extracted from a TRPM8 channel variant whose temperature dependence was decreased after CTD deletion—TRPM8ΔCT36—thus, the change in the free energy of folding of the CTD during cold-driven gating ($\Delta\Delta G^{T}_{CTD}$) is

$$\Delta\Delta G^{T}_{CTD} = \Delta\Delta G^{T}_{U,WT} - \Delta\Delta G^{T}_{U,\Delta CT36}. \qquad [8]$$

Using the data of Fig. 2 and Eq. **8** we obtain 1.44 ± 0.45 kcal/mol as the lower limit for the free energy change of the temperature-dependent folding of the CTD ($\Delta\Delta G^{T}_{CTD}$). Studies on soluble proteins have shown that the chemical unfolding ΔG of coiled coil domains with similar length ranges from 6 to 11 kcal/mol

(35–37). Therefore, the value of $\Delta\Delta G^{T}_{CTD}$ we obtained using Eq. **8** appears to be too small to involve the TRPM8 coiled coil domain in a folding–unfolding process in particular considering that the channel is a tetramer. However, we think that a small free energy change is predictable in this case because 1) in contrast to thermal/chemical denaturation, the TRPM8 channel gating requires complete reversibility of the closed–open reaction (i.e., an small $\Delta\Delta G^{T}_{CTD}$); 2) it is expected that as was reported for the heat receptor TRPV3 (38), temperature-dependent conformational changes at the CTD would be modest; and 3) our $\Delta\Delta G^{T}_{CTD}$ estimation is in excellent agreement with the ΔG ~1.6 kcal/mol of WT channel gating by cold (z ~0.7, ΔV_0 ~100 mV) (32, 39).

Solute-Inaccessible Aqueous Volume Changes at the C-Terminal Domain of the TRPM8 Channel. Proteins experience a decrease in their molar volume upon unfolding due to the loss of solute-excluded volume at the protein core (40–42). Changes in the solute-inaccessible aqueous volume during the gating of several ion channels have been determined before by quantifying the impact of exposing the protein to a large amount of a given osmoticant agent (43–47). Inspired by these studies, we devised a method to determine the temperature-dependent osmotic work performed by the channel CTD and, therefore, to estimate the change in its solute-inaccessible aqueous volume. If the channel can perform both electrical and osmotic work the addition of a large amount of sucrose will expose the channel to an additional osmotic work ΔW^{T}, which can be obtained as

$$\Delta W^{T} = zFV^{T}_{S} - zFV^{T}_{C}, \quad [9]$$

where zFV^{T}_{S} and zFV^{T}_{C} are the change in free energy of the closed–open transition in the presence of 2 M internal sucrose and in control recording solution, respectively. According to the results shown in Figs. 1 and 2 the CTD appears to be a major component of the temperature-sensing machinery of the TRPM8 channel. If this domain behaves as a bona fide temperature sensor, it would be expected to undergo a conformational change that may be accompanied by a change in its solute-inaccessible volume. In fashion analogous to our unfolding free energy measurements, we determined the temperature-dependent component of the osmotic work performed by the channel during the closed–open transition at 10 and 25 °C,

$$\Delta\Delta W^{T} = \Delta W^{10^{o}C} - \Delta W^{25^{o}C}. \quad [10]$$

In the simplest case in which we consider that the TRPM8 WT channel has a fully functional temperature sensor while that of the TRPM8ΔCT36 has been severely damaged, the osmotic work performed by the CTD as temperature varies between 25 and 10 °C is

$$\Delta\Delta W^{T}_{CTD} = (\Delta\Delta W^{T}_{WT} - \Delta\Delta W^{T}_{\Delta CT36}), \quad [11]$$

where $\Delta\Delta W^{T}_{WT}$ and $\Delta\Delta W^{T}_{\Delta CT36}$ are the temperature-dependent osmotic work performed by the WT and TRPM8ΔCT36 variants, respectively. As stated above, the osmotic work W is a function of the osmotic pressure and the change in the solute-inaccessible aqueous volume between the initial and final states of a given activation landscape (48). Thus, the temperature-dependent change in the solute-inaccessible aqueous volume of the CTD of the TRPM8 channel is

$$\Delta v^{T}_{CTD} = \frac{\Delta\Delta W^{T}_{CTD}}{(\Pi_S - \Pi_C)}, \quad [12]$$

where $\Delta\Delta W^{T}_{CTD}$ is the difference in the osmotic work performed by the CTD at 25 and 10 °C and Π_S and Π_C are the osmotic pressure in 2 M sucrose and control recording solutions, respectively. We recorded the TRPM8 WT channel and the reduced temperature sensitivity TRPM8ΔCT36 variant in the presence of 2 M internal sucrose at 10 and 25 °C. Fig. 3 *A–D* shows current traces evoked by voltage test pulses in membrane patches containing TRPM8 WT and TRPM8ΔCT36 in the presence of 2 M of internal sucrose at 10 °C (Fig. 3 *A* and *C*) and 25 °C (Fig. 3 *B* and *D*) and the respective G–V curves obtained using the normalized amplitude of the tail currents (Fig. 3 *E–H*). Boltzmann equation fit parameters for each TRPM8 channel variant/experimental condition can be found in *SI Appendix*, Table S1.

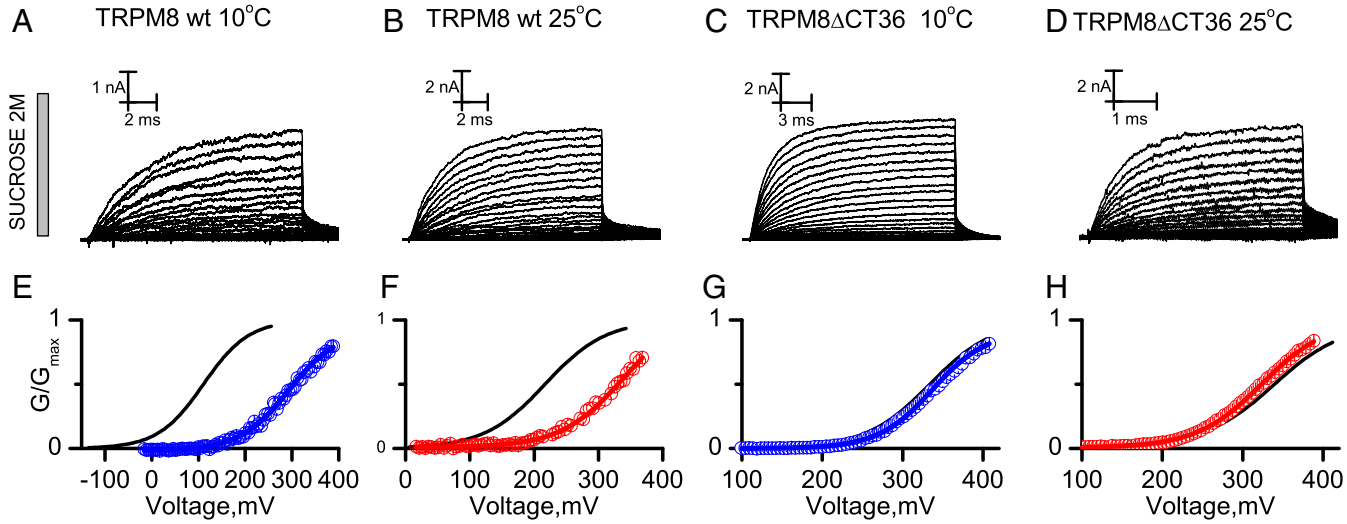

Fig. 3. Temperature-dependent changes in the solute-inaccessible aqueous volume of TRPM8 channels. Representative recordings of macroscopic currents of (*A* and *B*) TRPM8 and (*C* and *D*) TRPM8ΔCT36 channels in the presence of internal 2 M sucrose at 10 and 25 °C evoked by voltage pulses ranging between −140 and 420 mV in 5-mV increments. For the sake of clarity, only one of every two current records is shown in *A–D*. (*E–H*) Average G–V relationships obtained from normalized tail currents. Solid lines are Boltzmann fits to Eq. S1 (*SI Appendix*, Eq. S1). Blue open circles are data obtained at 10 °C, and red open circles are data obtained at 25 °C. Fit parameters are summarized in *SI Appendix*, Table S2. Detailed voltage protocols are given in *SI Appendix*, Table S3. Error bars are SE, $n = 4$ to 7.

Sucrose induced 205 ± 12 and 85 ± 13 mV rightward shifts in the G–V curve of TRPM8 WT channels at 10 and 25 °C, respectively (Fig.3 *E* and *F*), which, using Eq. **10**, is equivalent to osmotic works of 3.18 ± 0.20 and 1.25 ± 0.20 kcal/mol, respectively. The TRPM8ΔCT36 variant exhibited small sucrose-induced voltage shifts of 25 ± 9 and −13 ± 6 mV at 10 and 25 °C, respectively (Fig. 3 *G* and *H*), equivalent to osmotic works of 0.4 ± 0.13 and −0.20 ± 0.08 kcal/mol. The lack of change in the solute-inaccessible aqueous volume of TRPM8ΔCT36 between the closed and open states suggests that the difference in the osmotic work performed by the WT channel at 10 and 25 °C arises from the osmotic strain of preserving the CTD in the folded (10 °C) or unfolded (25 °C) states in the presence of the osmoticant. Thus, and according to Eq. **9**, the channel region encompassing the coiled coil domain and the linker that connect it with the carboxy helix 2 (CH2) domain performs a temperature-dependent osmotic work of 1.34 ± 0.32 kcal/mol, which, using Eq. **12**, represents a 1,906 ± 453 Å^3 increase in their solute-inaccessible aqueous volume.

Discussion

The Heat Capacity Hypothesis Revisited. Here we propose that the opening of the TRPM8 channel caused by cold requires the integrity of the CTD, which folds ($\Delta\Delta G^{T}_{CTD} = 1.44 \pm 0.45$ kcal/mol) and increases the solute-inaccessible aqueous volume ($\Delta v^{T}_{CTD} = 1{,}906 \pm 453$ Å^3) in response to cold. These conjectures are supported by the following facts: 1) the temperature dependence of the channel decreases after deleting the distal section of CTD, 2) exposing the intracellular side of the channel to urea stabilizes the closed state preferentially at low temperatures, 3) this effect is dependent on the integrity of the CTD and is therefore attenuated or absent in the TRPM8ΔCT36 variant, and 4) the temperature-dependent volume increase at the CTD (1,906 Å^3) is equivalent to the volume of the hollow space inside the CTD according to the Cryo-EM structure. We confront below our results with the current models of thermo-TRP channels gating. The unusually large temperature dependence of thermo-TRP channels activity has been satisfactorily explained—from a theoretical point of view—by large changes in the protein heat capacity (ΔCp) during the closed–open transition (19). One of the strengths of this model is that it makes the existence of a temperature sensor unnecessary and turns a problem that is usually treated as a complex network of allosteric interactions (32, 49, 50) into a protein denaturation matter. Additionally, the requirements of a temperature-sensing protein in terms of ΔCp can be achieved by changing the solvent exposure of ∼25 hydrophobic amino acids per subunit (19, 51), which is supported by the small structural changes between closed and open conformations reported in several thermo-TRPs (11, 38, 52, 53). In the context of the TRPM8 channel, the ΔCp hypothesis predicts that a conformational change, analogous to cold denaturation, drives the increase in the channel open probability at low temperatures. At first glance, our results are at odds with the ΔCp hypothesis mostly because the chemical unfolding of the channel CTD by urea hinders (instead of promoting) channel opening (Fig. 2) but does so mostly at low temperatures where, according to the ΔCp hypothesis, cold denaturation has already taken place. However, it is worth mentioning that cold denaturation is a rare phenomenon even for soluble proteins and, with a few notable exceptions (54, 55), occurs mostly in the presence of denaturing agents, supercooled fluids, high pressure, or extreme pH and ionic strength (56). Can our results be framed into the ΔC_p hypothesis? To answer this question, consider a system where a certain protein domain experiences a temperature-dependent unfolding:

$$F \overset{K(T)}{\Leftrightarrow} U, \qquad [13]$$

where F and U are the folded (F) and unfolded (U) states, whose equilibrium constant [K(T)] is determined by the Van't Hoff equation that incorporates the temperature dependence of ΔH and ΔS (19),

$$\ln K(T) = \frac{\Delta So}{R} - \frac{\Delta Cp\left[1 - \frac{To}{T} + \ln\left[\frac{To}{T}\right]\right]}{R}, \qquad [14]$$

where ΔSo is the difference of standard entropy between the resting and active state of the protein, ΔCp is the change in the molar heat capacity, and To is the temperature where $K = \frac{\Delta S_o}{R}$. Thus, we propose here that the F state increases the channel open probability (Po):

$$Po = \frac{1}{K(T) + 1}. \qquad [15]$$

Fig. 4*A* shows the open probability of the TRPM8 channel at +260 mV (Fig. 4*A*, *Left*), and the Po obtained very negative membrane potentials (Fig. 4*A*, *Right*)—potentials at which all of the voltage sensors are at rest—determined at temperatures

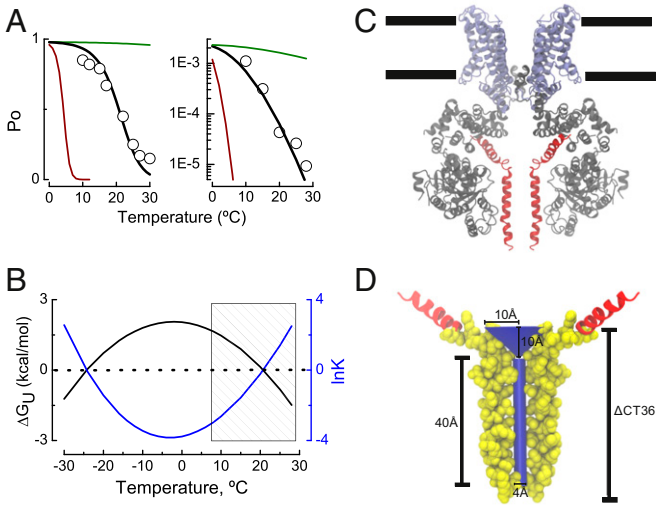

Fig. 4. A thermodynamically inspired–structure-supported model for TRPM8 channel gating. (*A*) TRPM8 channel open probability recorded at +260 mV (*Left*) and the minimal channel open probability recorded at very negative potentials using the limiting slope method (*Right*) at temperatures ranging from 10 to 30 °C according to ref. 32 (hollow circles). Black line represents the fit of Eqs. **14** and **15** to the experimental data from Raddatz et al. (32). Best fit parameters were ΔCp = 2.2 kcal/mol*K and ΔSo = −7.6 cal/molK (*Left*) and ΔCp = 2.2 kcal/mol*K and ΔSo = 12 cal/mol*K (*Right*). To = 270K (−3 °C) in both panels. The green and red lines in Fig. 1*A* are the Po values between 0 and 30 °C according to Eqs. **14** and **15** using ΔCp = 0.22 and 22 kcal/mol*K, respectively. (*B*) Difference in the free energy of unfolding ΔGU (kcal/mol) between resting–active state of the TRPM8 temperature sensor according to Eqs. **4** and **11** (fit parameters as in Fig. 4*A*, *Left*). Shaded area depicts the temperature range where the experiments in ref. 32 were performed. (*C*) Ligand-free TRPM8 structure obtained by spCryo-EM (PDB ID 6O6A; ref. 9), where the N terminus domain is colored in gray, transmembrane segments 1 to 6 and TRP domain appear in purple, and distal CTD is in red (subunits in the front and in the back were removed for clarity). Black lines define the approximate lipid bilayer limits. (*D*) The deleted CTD section (ΔCT36) allocates a 40 Å × 2 Å (length × radius) cylinder of volume 503 Å^3 plus a cone of 10 Å × 10 Å (radius × height), with a volume of 1,047 Å^3. The segment encompassing the 36 amino acids whose deletion decreases the channel temperature dependence (TRPM8ΔCT36) is depicted in Van der Waals representation using the Visual Molecular Dynamics (VMD) software (66).

ranging from 30 to 10 °C (32). The best fit to the Po-T data using Eqs. **14** and **15** was obtained with the following parameter values: $\Delta So = -7.6$ cal/mol*K, To = 270 K, and $\Delta Cp = 2.2$ kcal/mol*K (for Po data obtained at +260 mV) and $\Delta So = 12$ cal/mol*K, To = 270 K, and $\Delta Cp = 2.2$ kcal/mol*K (for Po data obtained at negative voltages). Additionally, panels in Fig. 4*A* include the Po values predicted by Eqs. **14** and **15** using a higher (22 kcal/mol*K; red curve) and lower (0.2 kcal/mol*K; green curve) ΔCp value. Fig. 4*B* shows the free energy of unfolding of the temperature-sensing domain, ΔG_U (kcal/mol) (black line, left ordinate), and the natural logarithm of the equilibrium constant that defines the folded/unfolded transition, lnK (blue line, right ordinate) vs. temperature obtained from Eqs. **14** and **2**. From Fig. 4*A* it is clear that the modified heat capacity model is able to predict the temperature dependence of the channel open probability with (Fig. 4*A*, *Left*) or without (Fig. 4*A*, *Right*) the free energy contribution of the voltage-sensing domain. Interestingly, the fit to both Po-T datasets using Eq. **14** reveals that channel entropy ΔS_o decreases by ∼20 cal/mol*K at depolarized membrane potentials. This finding is in agreement with the fact that the TRPM8 has a negative ΔS for the close-to-open transition (57). From the red and green lines in Fig. 4*A* and corresponding Eq. **14** with $\Delta Cp = 22$ kcal/mol*K (red line) and $\Delta Cp = 0.22$ kcal/mol*K (green line), it is evident that the TRPM8 channel does not tolerate large variations from the best fit obtained without departing from its characteristic temperature dependence. Fig. 4*B* shows that the current set of fit parameters required to reproduce the cold activation of TRPM8 channels is not compatible with cold denaturation, which is predicted to occur at temperatures below −20 °C. When we restrict our analysis to the working temperature range of the TRPM8 channel (Fig. 4*B*, hatched rectangle), we can observe that the unfolded state becomes less populated as temperature decreases. Surprisingly, the net free energy of folding ΔG_F between 30 and 10 °C obtained after fitting the data to Eqs. **3** and **14** is ∼2 kcal/mol, which is in a reasonable agreement with the 1.44 ± 0.45 kcal/mol we found for the temperature-dependent folding of the TRPM8 CTD.

Thus, the changes in the molar heat capacity are likely to drive the gating of the TRPM8 channel with the sole requirement of an inverted coupling between the temperature sensor denaturation and channel opening (58). Inverted coupling is not alien to ion channel biophysics and accounts for some important features of Kv channels where electromechanical coupling and gating polarity is reverse (59, 60), and inactivation (61). Inverted coupling is also found in thermo-TRP channels gating, where reversion of the temperature dependence has been achieved after swapping the C/N terminus (27, 62) and by single-point mutations in both the amino and the carboxyl terminus domains (63).

Changes in the Solute-Inaccessible Aqueous Volume at the CTD. Volumetric changes have been reported before for several voltage-gated ion channels (43–47). By using a subtractive method (46) that takes advantage of the large decrease in the temperature sensitivity of the TRPM8ΔCT36 channel variant, we show that the CTD of the TRPM8 channel experiences a temperature-dependent change in their solute-inaccessible aqueous volume of ∼1,906 Å^3. According to the Cryo-EM structure [Protein Data Bank (PDB) ID 6O6A (9)] the region that TRMP8ΔCT36 lacks comprises amino acids 1094 to 1058, which includes the coiled coil domain and the loop connecting this region with the CTH2 helix (colored in red in Fig. 4*C*). The void volume inside the coiled coil domain can be represented by a 40 Å × 4 Å (length × diameter) cylinder with a volume of 503 Å^3. The inner space delimited by the coiled coil/CTH2 linker of the four subunits can be drawn as a 10 Å × 10 Å (length × radius) inverted cone, with a volume of volume of 1,047 Å^3 (Fig. 4*D*). If this were the folded state of the CTD, its inner volume of 1,550 Å^3 is in agreement with the appearance of a solute-inaccessible void space of 1,906 ± 453 Å^3, which our experiments under hyperosmotic conditions suggest occurs during the unfolding→folding transition (Fig. 3). From a physicochemical perspective, the distal CTD domain contains seven Leu/Ile residues/per subunit, all of them hidden from the solvent in the protein folded state (15). Supposing that each of them becomes totally exposed during protein unfolding (F→U), the molar heat capacity increases by ∼5 to 11 kcal/mol*K (64). In this scenario, a moderate increase in the solvent exposure of 20 to 50% would provide the ΔCp necessary to qualitatively reproduce the temperature dependence of the TRPM8 channel gating (2.2 kcal/mol*K; Fig. 4*A*). Here we propose that the temperature-driven gating of TRPM8 channel arises from the change in the molar heat capacity occurring during the unfolding of a discrete temperature sensor located at the CTD, which folds in response to cold and increases its solute-inaccessible aqueous volume between the unfolded–folded states. Although these results provide compelling evidence regarding the operating mechanism during the TRPM8 temperature-driven gating, the intimacies of the molecular timing of the fating events remain elusive. Interestingly, all members of the TRPM channel class are endowed with similar CTD including warm/hot receptors (TRPM3, TRPM4, and TRPM5) and temperature-insensitive channels (TRPM6 and TRPM7) (65). Thus, the role of the CTD in heat sensing and how the thermomechanical coupling varies across the members of the thermo-TRPM channel family remains a pending issue for the thermo-TRP channels field.

Materials and Methods

Oocyte Extraction and RNA Injection. *Xenopus laevis* oocytes were obtained and injected with 50 nL of RNA at a concentration of 1 μg/μL and were then maintained at 18 °C in ND96 medium, which ensured 90% survival (32).

Site-Directed Mutagenesis, Channel Expression, and Electrophysiology. All TRPM8 variants were generated as in ref. 32. All experiments were performed using the patch clamp technique, and ionic currents were recorded using an Axopatch 200B amplifier and were digitized using a Digidata 1440 interface under control of pClamp 10 (Molecular Devices) at a sampling frequency of 50 to 200 kHz and filtered at 20 kHz. Characterization of the temperature dependence of the TRPM8 channels and their truncated CTD variants ΔCT8, ΔCT15, and ΔCT36 (Fig. 1) was performed in the cell-attached configuration. Pipette and bath recording solution composition was (in mM) 110 KMES, 1 $MgCl_2$, 2 KCl, and 10 EGTA. Experiments in Figs. 2 and 3 were performed in the inside-out configuration. Both bath and pipette recording solution composition was (in mM) 110 NaCl, 1$MgCl_2$, and 10 EGTA. For experiments in the presence of a denaturing agent and hyperosmotic conditions the recording solution was supplemented with 3 M Urea and 2 M Sucrose, respectively. After seal formation the patch was excised, and the recording chamber was perfused with 3 to 5 times the total volume (2 mL) immediately after reaching the inside-out configuration. Temperature control was provided by a Dagan TC-10 temperature controller (Dagan Corp.). *SI Appendix, SI Methods*, includes the details of macroscopic current recordings and data analysis.

Data Availability. All study data are included in the article and *SI Appendix*.

ACKNOWLEDGMENTS. We thank Christopher Miller and John Ewer for comments on the manuscript and Mrs. Luisa Soto, Mr. Patricio Farias, and Mrs. Victoria Prado (Universidad de Valparaiso) for their excellent technical assistance. This research was supported by the Fondo Nacional de Desarrollo Científico y Tecnológico (FONDECYT) Regular 1190203 (to R.L.), 1170733 (to F.G.-N.), and 1180999 (to K.C.) and FONDECYT Postdoctorado 3170599 (to I.D.-F.), Proyecto PAI7719087 (to I.D.-F.); US Army Research Office Cooperative Agreement W911NF-17-2-0081 (to F.G.-N.); and US Air Force Office of Scientific Research grant under award FA9550-16-1-0384 (R.L.). The Centro Interdisciplinario de Neurociencias de Valparaiso (CINV) is a Millennium Institute supported by the Iniciativa Científica Milenio-Agencia Nacional de Investigación y Desarrollo (ICM-ANID), Project P09-022-F, CINV.

1. T. Voets, K. Talavera, G. Owsianik, B. Nilius, Sensing with TRP channels. *Nat. Chem. Biol.* **1**, 85–92 (2005).
2. Q. Feng, Temperature sensing by thermal TRP channels: Thermodynamic basis and molecular insights. *Curr. Top. Membr.* **74**, 19–50 (2014).
3. D. E. Clapham, L. W. Runnels, C. Strübing, The TRP ion channel family. *Nat. Rev. Neurosci.* **2**, 387–396 (2001).
4. Y. Liu, N. Qin, TRPM8 in health and disease: Cold sensing and beyond. *Adv. Exp. Med. Biol.* **704**, 185–208 (2011).
5. T. Voets *et al*., The principle of temperature-dependent gating in cold- and heat-sensitive TRP channels. *Nature* **430**, 748–754 (2004).
6. B. Liu, F. Qin, Functional control of cold- and menthol-sensitive TRPM8 ion channels by phosphatidylinositol 4,5-bisphosphate. *J. Neurosci.* **25**, 1674–1681 (2005).
7. T. Rohács, C. M. Lopes, I. Michailidis, D. E. Logothetis, PI(4,5)P2 regulates the activation and desensitization of TRPM8 channels through the TRP domain. *Nat. Neurosci.* **8**, 626–634 (2005).
8. A. M. Peier *et al*., A TRP channel that senses cold stimuli and menthol. *Cell* **108**, 705–715 (2002).
9. M. M. Diver, Y. Cheng, D. Julius, Structural insights into TRPM8 inhibition and desensitization. *Science* **365**, 1434–1440 (2019).
10. I. Erler *et al*., Trafficking and assembly of the cold-sensitive TRPM8 channel. *J. Biol. Chem.* **281**, 38396–38404 (2006).
11. E. Cao, M. Liao, Y. Cheng, D. Julius, TRPV1 structures in distinct conformations reveal activation mechanisms. *Nature* **504**, 113–118 (2013).
12. C. E. Paulsen, J. P. Armache, Y. Gao, Y. Cheng, D. Julius, Structure of the TRPA1 ion channel suggests regulatory mechanisms. *Nature* **520**, 511–517 (2015).
13. L. Zubcevic *et al*., Cryo-electron microscopy structure of the TRPV2 ion channel. *Nat. Struct. Mol. Biol.* **23**, 180–186 (2016).
14. A. K. Singh, L. L. McGoldrick, A. I. Sobolevsky, Structure and gating mechanism of the transient receptor potential channel TRPV3. *Nat. Struct. Mol. Biol.* **25**, 805–813 (2018).
15. Y. Yin *et al*., Structure of the cold- and menthol-sensing ion channel TRPM8. *Science* **359**, 237–241 (2018).
16. M. García-Ávila, L. D. Islas, What is new about mild temperature sensing? A review of recent findings. *Temperature* **6**, 132–141 (2019).
17. I. Diaz-Franulic, H. Poblete, G. Miño-Galaz, C. González, R. Latorre, Allosterism and structure in thermally activated transient receptor potential channels. *Annu. Rev. Biophys.* **45**, 371–398 (2016).
18. L. D. Islas, "Molecular mechanisms of temperature gating in TRP channels" in *Neurobiology of TRP Channels*, T. L. R. Emir, Ed. (Press/Taylor & Francis, Boca Raton, FL, 2017), pp. 11–25.
19. D. E. Clapham, C. Miller, A thermodynamic framework for understanding temperature sensing by transient receptor potential (TRP) channels. *Proc. Natl. Acad. Sci. U.S.A.* **108**, 19492–19497 (2011).
20. L. Moparthi *et al*., Human TRPA1 is a heat sensor displaying intrinsic U-shaped thermosensitivity. *Sci. Rep.* **6**, 28763 (2016).
21. O. Gal-Mor, Y. Valdez, B. B. Finlay, The temperature-sensing protein TlpA is repressed by PhoP and dispensable for virulence of Salmonella enterica serovar Typhimurium in mice. *Microbes Infect.* **8**, 2154–2162 (2006).
22. E. Saita *et al*., A coiled coil switch mediates cold sensing by the thermosensory protein DesK. *Mol. Microbiol.* **98**, 258–271 (2015).
23. D. I. Piraner, Y. Wu, M. G. Shapiro, Modular thermal control of protein dimerization. *ACS Synth. Biol.* **8**, 2256–2262 (2019).
24. C. Arrigoni *et al*., Unfolding of a temperature-sensitive domain controls voltage-gated channel activation. *Cell* **164**, 922–936 (2016).
25. Y. Fujiwara, Y. Okamura, Temperature-sensitive gating of voltage-gated proton channels. *Curr. Top. Membr.* **74**, 259–292 (2014).
26. C. Arrigoni, D. L. Minor Jr., Global versus local mechanisms of temperature sensing in ion channels. *Pflugers Arch.* **470**, 733–744 (2018).
27. S. Brauchi, G. Orta, M. Salazar, E. Rosenmann, R. Latorre, A hot-sensing cold receptor: C-terminal domain determines thermosensation in transient receptor potential channels. *J. Neurosci.* **26**, 4835–4840 (2006).
28. F. H. Crick, Is alpha-keratin a coiled coil? *Nature* **170**, 882–883 (1952).
29. A. N. Lupas, M. Gruber, The structure of alpha-helical coiled coils. *Adv. Protein Chem.* **70**, 37–78 (2005).
30. E. O. Gracheva *et al*., Ganglion-specific splicing of TRPV1 underlies infrared sensation in vampire bats. *Nature* **476**, 88–91 (2011).
31. Y. Fujiwara *et al*., The cytoplasmic coiled-coil mediates cooperative gating temperature sensitivity in the voltage-gated H(+) channel Hv1. *Nat. Commun.* **3**, 816 (2012).
32. N. Raddatz, J. P. Castillo, C. Gonzalez, O. Alvarez, R. Latorre, Temperature and voltage coupling to channel opening in transient receptor potential melastatin 8 (TRPM8). *J. Biol. Chem.* **289**, 35438–35454 (2014).
33. S. Brauchi, P. Orio, R. Latorre, Clues to understanding cold sensation: Thermodynamics and electrophysiological analysis of the cold receptor TRPM8. *Proc. Natl. Acad. Sci. U.S.A.* **101**, 15494–15499 (2004).
34. P. L. Privalov, Stability of proteins: Small globular proteins. *Adv. Protein Chem.* **33**, 167–241 (1979).
35. J. R. Litowski, R. S. Hodges, Designing heterodimeric two-stranded alpha-helical coiled-coils. Effects of hydrophobicity and alpha-helical propensity on protein folding, stability, and specificity. *J. Biol. Chem.* **277**, 37272–37279 (2002).
36. H. Chao *et al*., Kinetic study on the formation of a de novo designed heterodimeric coiled-coil: Use of surface plasmon resonance to monitor the association and dissociation of polypeptide chains. *Biochemistry* **35**, 12175–12185 (1996).
37. G. De Crescenzo, J. R. Litowski, R. S. Hodges, M. D. O'Connor-McCourt, Real-time monitoring of the interactions of two-stranded de novo designed coiled-coils: Effect of chain length on the kinetic and thermodynamic constants of binding. *Biochemistry* **42**, 1754–1763 (2003).
38. A. K. Singh *et al*., Structural basis of temperature sensation by the TRP channel TRPV3. *Nat. Struct. Mol. Biol.* **26**, 994–998 (2019).
39. B. Nilius *et al*., Gating of TRP channels: A voltage connection? *J. Physiol.* **567**, 35–44 (2005).
40. N. Ando *et al*., Structural and thermodynamic characterization of T4 lysozyme mutants and the contribution of internal cavities to pressure denaturation. *Biochemistry* **47**, 11097–11109 (2008).
41. M. D. Collins, G. Hummer, M. L. Quillin, B. W. Matthews, S. M. Gruner, Cooperative water filling of a nonpolar protein cavity observed by high-pressure crystallography and simulation. *Proc. Natl. Acad. Sci. U.S.A.* **102**, 16668–16671 (2005).
42. K. J. Frye, C. A. Royer, Probing the contribution of internal cavities to the volume change of protein unfolding under pressure. *Protein Sci.* **7**, 2217–2222 (1998).
43. J. Zimmerberg, V. A. Parsegian, Polymer inaccessible volume changes during opening and closing of a voltage-dependent ionic channel. *Nature* **323**, 36–39 (1986).
44. J. Zimmerberg, F. Bezanilla, V. A. Parsegian, Solute inaccessible aqueous volume changes during opening of the potassium channel of the squid giant axon. *Biophys. J.* **57**, 1049–1064 (1990).
45. X. Jiang, G. C. Bett, X. Li, V. E. Bondarenko, R. L. Rasmusson, C-type inactivation involves a significant decrease in the intracellular aqueous pore volume of Kv1.4 K+ channels expressed in Xenopus oocytes. *J. Physiol.* **549**, 683–695 (2003).
46. I. Díaz-Franulic, V. González-Pérez, H. Moldenhauer, N. Navarro-Quezada, D. Naranjo, Gating-induced large aqueous volumetric remodeling and aspartate tolerance in the voltage sensor domain of Shaker K^+ channels. *Proc. Natl. Acad. Sci. U.S.A.* **115**, 8203–8208 (2018).
47. F. Kukita, Solvent effects on squid sodium channels are attributable to movements of a flexible protein structure in gating currents and to hydration in a pore. *J. Physiol.* **522**, 357–373 (2000).
48. J. Zimmerberg, V. A. Parsegian, Water movement during channel opening and closing. *J. Bioenerg. Biomembr.* **19**, 351–358 (1987).
49. J. A. Matta, G. P. Ahern, Voltage is a partial activator of rat thermosensitive TRP channels. *J. Physiol.* **585**, 469–482 (2007).
50. L. Gregorio-Teruel, P. Valente, J. M. González-Ros, G. Fernández-Ballester, A. Ferrer-Montiel, Mutation of I696 and W697 in the TRP box of vanilloid receptor subtype I modulates allosteric channel activation. *J. Gen. Physiol.* **143**, 361–375 (2014).
51. F. Qin, Demystifying thermal channels: Driving a channel both forwards and backwards with a single gear? *Biophys. J.* **104**, 2118–2120 (2013).
52. L. Wang *et al*., Structures and gating mechanism of human TRPM2. *Science* **362**, eaav4809 (2018).
53. L. L. McGoldrick *et al*., Structure of the thermo-sensitive TRP channel TRP1 from the alga Chlamydomonas reinhardtii. *Nat. Commun.* **10**, 4180 (2019).
54. A. Pastore *et al*., Unbiased cold denaturation: Low- and high-temperature unfolding of yeast frataxin under physiological conditions. *J. Am. Chem. Soc.* **129**, 5374–5375 (2007).
55. J. R. Bothe *et al*., The complex energy landscape of the protein IscU. *Biophys. J.* **109**, 1019–1025 (2015).
56. P. L. Privalov, Cold denaturation of proteins. *Crit. Rev. Biochem. Mol. Biol.* **25**, 281–305 (1990).
57. A. M. Correa, F. Bezanilla, R. Latorre, Gating kinetics of batrachotoxin-modified Na+ channels in the squid giant axon. Voltage and temperature effects. *Biophys. J.* **61**, 1332–1352 (1992).
58. A. Jara-Oseguera, L. D. Islas, The role of allosteric coupling on thermal activation of thermo-TRP channels. *Biophys. J.* **104**, 2160–2169 (2013).
59. R. Männikkö, F. Elinder, H. P. Larsson, Voltage-sensing mechanism is conserved among ion channels gated by opposite voltages. *Nature* **419**, 837–841 (2002).
60. R. Latorre *et al*., Molecular coupling between voltage sensor and pore opening in the Arabidopsis inward rectifier K+ channel KAT1. *J. Gen. Physiol.* **122**, 459–469 (2003).
61. A. J. Labro, D. M. Cortes, C. Tilegenova, L. G. Cuello, Inverted allosteric coupling between activation and inactivation gates in K^+ channels. *Proc. Natl. Acad. Sci. U.S.A.* **115**, 5426–5431 (2018).
62. J. F. Cordero-Morales, E. O. Gracheva, D. Julius, Cytoplasmic ankyrin repeats of transient receptor potential A1 (TRPA1) dictate sensitivity to thermal and chemical stimuli. *Proc. Natl. Acad. Sci. U.S.A.* **108**, E1184–E1191 (2011).
63. S. Jabba *et al*., Directionality of temperature activation in mouse TRPA1 ion channel can be inverted by single-point mutations in ankyrin repeat six. *Neuron* **82**, 1017–1031 (2014).
64. G. I. Makhatadze, P. L. Privalov, Heat capacity of proteins. I. Partial molar heat capacity of individual amino acid residues in aqueous solution: Hydration effect. *J. Mol. Biol.* **213**, 375–384 (1990).
65. Y. Huang, R. Fliegert, A. H. Guse, W. Lü, J. Du, A structural overview of the ion channels of the TRPM family. *Cell Calcium* **85**, 102111 (2020).
66. W. Humphrey, A. Dalke, K. Schulten, VMD: Visual molecular dynamics. *J. Mol. Graph* **14**, 33–38, 27–38 (1996).